JOURNAL OF MATERIALS SCIENCE 39 (2004) 2349–2356

Characterization of cerium and copper species in Cu—Ce—Al oxide systems by temperature programmed reduction and electron paramagnetic resonance

C. DECARNE, E. ABI-AAD*
Laboratoire de Catalyse et Environnement, E. A. 2598, Université du Littoral-Côte d'Opale, 145 avenue Maurice Schumann, 59140 Dunkerque, France
E-mail: abiaad@univ-littoral.fr

B. G. KOSTYUK, V. V. LUNIN
Laboratory of Catalysis and Gas Electrochemistry, Chemistry Department, M. V. Lomonosov Moscow State University, 119899 Vorobjevy Gory, Moscow B-234, Russia

A. ABOUKAÏS
Laboratoire de Catalyse et Environnement, E. A. 2598, Université du Littoral-Côte d'Opale, 145 avenue Maurice Schumann, 59140 Dunkerque, France

The reducibility of Ce–Al–O and Cu–Ce–Al–O solids is studied by H_2-TPR and EPR in order to identify the different ceria and copper oxide species. The study of Ce–Al–O oxides shows that dispersion of ceria on alumina improves reducibility of ceria bulk and stabilizes surface ceria. Concerning quantitative results, ceria reduction extent is more important for Ce–Al–O oxides than for pure ceria. This result can be related to the dispersion of ceria on alumina which decreases ceria crystallites size and enhances the ceria bulk reduction. For ternary oxides, copper oxide and ceria interact strongly. Introduction of copper facilitated ceria reduction, and quantitatively, the presence of copper favors the total reduction of ceria contrary to Ce–Al–O oxides. When ceria loading is low, two copper species are identified, and are attributed to small clusters and highly dispersed copper oxides. During the reduction of copper species, a partial reduction of ceria is observed. Increasing of copper loading leads to the formation of CuO aggregates.

1. Introduction

Elaboration of automobile catalysts for diesel engine is one of the most important environmental problems of these last decades. CeO_2 is widely used as a promoter in current based automobile catalysts. Three main properties make ceria an essential component in such redox catalysts: its oxygen storage capacity (OSC) [1]; its redox properties (Ce^{4+}/Ce^{3+}) and its thermal stabilizing influence on alumina [2–4]. Copper oxide is a well-known component of catalysts for a lot of reaction, as CO [5–11], volatile organic compounds (VOC) [12, 13] or CH_4 [8, 9] oxidation, NO_x reduction [11, 14–16] or soot combustion [17–22]. For automotive catalysts, copper is an interesting substitute to noble metal because of its catalytic properties and its cost. Copper can exist on different forms (isolated Cu^{2+} ions, highly dispersed clusters, small clusters and CuO aggregates), and depending on the reaction, one of these species is more interesting than the others. According to literature data, isolated copper ions are the most active copper species for CH_4 oxidation [9] whereas for CO oxidation, small clusters are the most active copper species [9, 10]. For decomposition of nitrous oxide (N_2O), isolated copper has little effect on activity, whereas small clusters seem to be the most active copper species [15]. Concerning soot combustion, aggregates seem more active than isolated copper species [20]. Thus, it is very interesting to know the copper species distribution on solid in order to explain the behavior of catalysts versus oxidation reactions. The aim of this work is to study the reduction of Ce—Al—O and Cu—Ce—Al—O solids, to know the influence of both copper oxide and ceria on the reduction of the system and the influence of their loading on copper dispersion.

2. Experimental

2.1. Solids preparation

Alumina is synthesized by sol-gel method. Secondary aluminum butylate ($Al(OC_4H_9)_3$, Fluka, ~11.0 wt%

*Author to whom all correspondence should be addressed.

TABLE I Ce—Al—O and Cu—Ce—Al—O samples composition and specific area after calcination at 600°C

	wt% of CuO	wt% of CeO_2	Specific area (m^2/g)	Calculated specific area (m^2/g)	Atomic composition
Al_2O_3	–	–	420	(420)	Al_2O_3
1Ce10Al	–	26.2%	301	(324)	$Ce_{1.05}Al_{10}O_{17.1}$
3Ce10Al	–	51.0%	212	(234)	$Ce_{3.08}Al_{10}O_{21.16}$
10Ce10Al	–	75.8%	149	(143)	$Ce_{9.28}Al_{10}O_{33.56}$
CeO_2	–	*100%*	55	(55)	CeO_2
1Cu10Al	16.4%	–	351	(352)	$Cu_{1.26}Al_{10}O_{16.26}$
1Cu1Ce10Al	10.8%	23.3%	277	(290)	$Cu_{1.05}Ce_{1.05}Al_{10}O_{18.15}$
1Cu3Ce10Al	6.6%	47.6%	192	(219)	$Cu_{0.92}Ce_{3.08}Al_{10}O_{22.08}$
5Cu3Ce10Al	25.6%	38.1%	152	(175)	$Cu_{4.53}Ce_{3.11}Al_{10}O_{25.75}$
1Cu10Ce10Al	3.6%	73.1%	110	(138)	$Cu_{0.98}Ce_{9.28}Al_{10}O_{34.54}$
5Cu10Ce10Al	*15.1%*	*65.5%*	98	(119)	$Cu_5Ce_{10}Al_{10}O_{40}$
1Cu10Ce	4.4%	95.6%	47	(53)	$Cu_{0.99}Ce_{10}O_{20.99}$

Italics: calculated wt% values.

Al) is dissolved in butan-2-ol (Fluka, purity ≥99.5%). Then, complexing agent (Butan-1,3-diol, Fluka, purity ≥98%) is added before hydrolysis [23]. Alumina is calcined at 500°C for 4 h before used as support for preparing supported catalysts. With this method alumina is partially crystallized under γ form.

Ceria is prepared by precipitation of $Ce(NO_3)_3 \cdot 6H_2O$ (Prolabo, total amount of rare earth oxides is 99.5%) in an ammonia aqueous solution (0.7 mol/L). The solid is filtered, washed, dried at 100°C and calcined at 600°C for 4 h with a temperature rate of 0.5°C/min.

Different Ce—Al—O oxides are prepared by incipient wetness of cerium nitrate solution onto alumina pre-calcined at 500°C. Then, the sample is dried at 100°C and calcined for 4 h in a flow of dry air at 600°C. Cerium containing solids are denoted 1Ce10Al, 3Ce10Al and 10Ce10Al, where the number before chemical symbol represents the atomic content in the solid.

Copper containing solids are prepared by incipient wetness of a support calcined at 500°C (aluminum, cerium or Ce—Al oxides) with aqueous solution of copper nitrate ($Cu(NO_3)_3 \cdot 3H_2O$, Prolabo, purity ≥99.0%). The mixture is dried at 100°C and calcined at 600°C for 4 h in a flow of dry air. Copper containing solids are denoted as supports, 0.5Cu10Al, 1Cu10Al, 1Cu1Ce10Al, 1Cu3Ce10Al, 5Cu3Ce10Al, 1Cu10Ce10Al, 5Cu10Ce10Al and 1Cu10Ce.

Table I summarizes composition of supports and copper containing catalysts performed in the central elementary analysis office of the CNRS (Vernaison).

2.2. Specific area

Specific area measurements are performed using a Quantasorb Junior System (Ankerschmidt). Approximately 30 mg of catalyst are outgassed in a flow of helium at 130°C for 30 min prior to adsorption measurements. Adsorption is made with a N_2/He mixture (30% N_2) at −196°C. With this one-point method, the accuracy of specific area is about 10%.

Table I shows specific area obtained for supports and copper based catalysts calcined at 600°C. In parallel, theoretical values are calculated from specific area of simple oxides (Al_2O_3, CeO_2 and CuO calcined at 600°C) and their weight percentage in the considered solid. Sol-gel synthesized alumina has a high specific area of 420 m^2/g. Specific area of ceria and copper oxide are respectively 55 and 8 m^2/g.

2.3. Temperature programmed reduction (TPR)

Temperature programmed reduction (TPR) of samples is carried out in a flow device equipped with a system of gas preparation and purification, a quartz reactor, a tube furnace and a thermal conductivity detector (TCD). All solids used for TPR experiments were previously calcined at 600°C. Before the TPR measurements, the solids are activated at 450°C under an oxygen flow for 1 h. A typical reduction is performed on 50 mg of sample in a mixture of 5 vol% H_2 in Ar. The flow rate is 23 mL/min and the heating rate is 13.2°C/min. H_2 consumption is estimated by comparison of the integrated peak areas with those obtained for standard (NiO). Integration is performed after the correction of the baseline of each TPR peak. The area of the TPR (related to quantity of labile oxygen) and the temperature of maximal reduction (characteristic of oxygen mobility) are chosen as parameters used for interpretation of TPR data on the redox properties of solids.

2.4. Electron paramagnetic resonance (EPR)

The electron paramagnetic resonance (EPR) measurements are performed at −196°C on a EMX BRUKER spectrometer equipped with a cavity operating at a frequency of ∼9.5 GHz (X band). The magnetic field was modulated at 100 kHz. The *g* values are determined from precise frequency and magnetic field values. EPR intensity is given by the normalized double integration of the EPR signal.

3. Results and discussion

3.1. Ce–Al–O samples

Four supports are studied: Al_2O_3, 1Ce10Al, 10Ce10Al and CeO_2. Hydrogen consumption curves are presented in Fig. 1.

For alumina, no hydrogen peak is observed. Indeed, alumina is well known to be stable versus H_2 reduction.

The TPR profile of CeO_2 shows 3 peaks (Fig. 1). The first peak centered at 416°C is due to removal

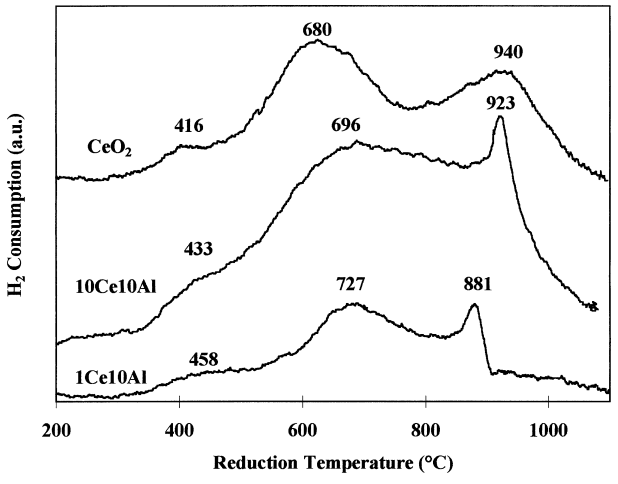

Figure 1 TPR profiles of Ce–Al–O samples.

of adsorbed oxygen on ceria [24]. Both major peaks centered at 680 and 940°C are attributed respectively to surface and bulk ceria reduction into Ce_2O_3 [1, 25, 26].

$$2CeO_2 + H_2 \rightarrow Ce_2O_3 + H_2O \qquad (1)$$

For mixed oxides, TPR profiles show 3 peaks as for pure ceria, due to adsorbed oxygen removal, surface and bulk ceria reduction. The removal of adsorbed oxygen needs lower temperature with increasing of ceria contents (Fig. 1). Indeed, for low ceria loading, ceria is highly stabilized and removal of adsorbed oxygen occurs at 458°C (1Ce10Al sample). This temperature decreases with increasing of ceria loading and passes to 433°C for 10Ce10Al sample and reaches a minimum of 416°C for pure ceria.

In the same order, surface ceria reduction takes place at lower temperature for pure ceria than for Ce–Al–O oxides. As for adsorbed oxygen removal, low ceria loading stabilizes surface ceria and the reduction takes place at 727°C for 1Ce10Al sample. With increasing of ceria content, surface ceria are less stabilized and temperature of reduction decreases to 696°C for 10Ce10Al sample and to 680°C for pure ceria.

Bulk reduction peak is observed on each sample, even on 1Ce10Al sample, showing a saturation of ceria dispersion. Indeed, the lowest content of ceria in our mixed oxides is 26.2 wt% (for 1Ce10Al), and according to literature data [1], bulk ceria reduction peak is observed from about 6 wt% of ceria. Furthermore, when ceria content increases, bulk ceria reduction is more difficult to occur, and needs higher temperature of reduction. Thus, bulk ceria reduction takes place at 881°C in the case of 1Ce10Al sample, whereas, it occurs at 940°C for pure ceria. Those results are in good agreements with those of Appel *et al.* [26], showing that increasing of ceria content leads to higher temperature of reduction of bulk ceria. Moreover, concerning bulk ceria reduction, the peak shape is different for pure ceria and mixed oxides. For pure ceria, reduction peak is broad, whereas for mixed oxides, the reduction peak of bulk ceria is well resolved and sharper, showing that hydrogen diffusion is easier for mixed oxides than for pure ceria.

Concerning quantitative results, if the complete reduction of ceria is achieved, the amount of hydrogen calculated from Equation 1 is 2.90 mmol per gram of ceria. Using this theoretical value, ceria reduction extents are calculated for each sample. Thus, for pure ceria, only 67 wt% of ceria are reduced. Bulk ceria is hardly reductible thus it is possible that bulk ceria cannot be entirely reduced in these experimental conditions. For 10Ce10Al, ceria reduction extents is 83 wt%. This increase of ceria reduction extent is probably due to better accessibility of bulk ceria. However, for 1Ce10Al sample, the ceria reduction extent is 68 wt%. In this case, the low value may be ascribable to better stabilization of surface ceria.

To summarize, pure ceria presents three peaks of reduction due to respectively removal of adsorbed oxygen, surface and bulk ceria reduction. For ceria dispersed on alumina, removal of adsorbed oxygen and surface ceria reduction need higher temperature to be achieved than pure ceria. On the contrary, bulk ceria reduction is facilitated when dispersed on alumina. Those phenomena are enhanced with decreasing of ceria content.

3.2. Cu–Ce–Al–O samples

Fig. 2 shows hydrogen consumption curves obtained for 1Cu10Al, 0.5Cu10Al, 1Cu10Ce, 1Cu1Ce10Al, 1Cu3Ce10Al, 1Cu10Ce10Al, 5Cu3Ce10Al and 5Cu10Ce10Al samples. Assuming that all copper species are reduced as followed:

$$CuO + H_2 \rightarrow Cu^0 + H_2O \qquad (2)$$

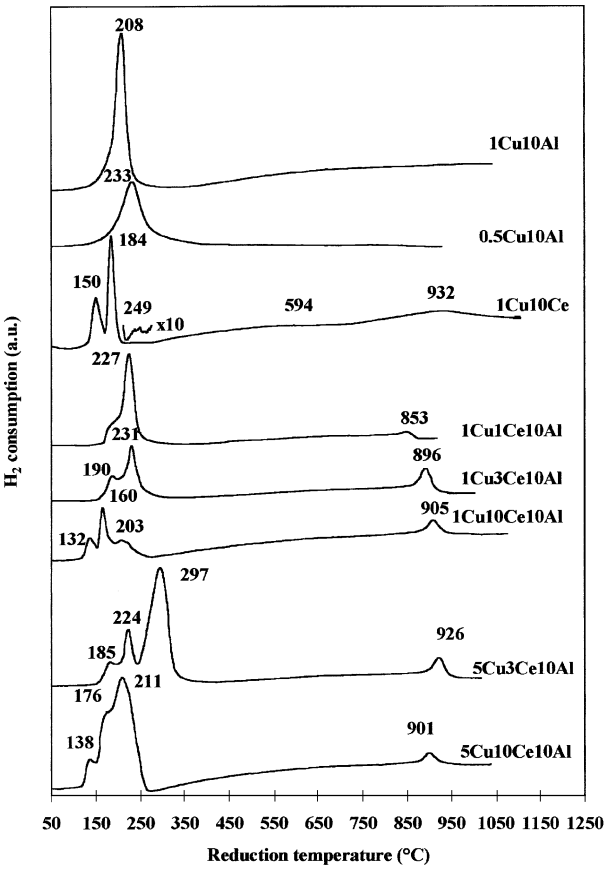

Figure 2 TPR profiles of copper based catalysts.

copper reduction extents are calculated from Equation 2 and from weight percent of copper oxide (Table I) for each sample.

TPR profile of 1Cu10Al sample shows a single peak centered at 208°C. According to literature data [13, 14, 27–31], this peak is attributed to the reduction of highly dispersed copper oxide species, which include isolated copper ions and well dispersed clusters. No bulk copper reduction is observed. Indeed, bulk copper reduction peak occurs from about 5 wt% of CuO per 100 m^2/g of alumina support [27–29] or 6 wt% of CuO per 100 m^2/g of ceria support [10, 32]. In this case (1Cu10Al), the amount of copper oxide is $\frac{16.4(wt\%)}{0.836\times420(m^2/g)} \times 100 = 4.7$ wt% per 100 m^2/g of support, where 16.4 represents the weight percent of copper oxide in the solid, 420 the specific area of alumina support and 0.836 the alumina loading in the solid. Consequently, the high dispersion of copper in 1Cu10Al sample allows to obtain only dispersed copper species. To confirm this result, EPR spectrum of 1Cu10Al is recorded at −196°C (Fig. 3). The spectrum shows two signals of copper species. The first signal with hyperfine structure is characteristic of Cu^{2+} ions with an axial symmetry [33–35]. The EPR parameters of this axial signal are: $g_{//} = 2.326$; $g_{\perp} = 2.054$; $A_{//} = 128$G; $A_{\perp} = 39$G. The other signal is isotropic, centered at $g_{iso} = 2.140$ with a line width $\triangle H_{pp} = 400$G and can be assigned to small clusters of copper ions [33, 34, 36, 37]. When the copper content is 2 times lower (0.5Cu10Al), the isotropic signal presents a sharper line width ($\triangle H_{pp} = 273$G) than 1Cu10Al sample (Fig. 3) and thus the relative intensity is significantly lower, while the total intensity of the 0.5Cu10Al sample is ∼2 times higher than 1Cu10Al sample (Table II), showing that copper is mainly under isolated Cu^{2+} ions. Moreover, TPR study of 0.5Cu10Al shows that copper reduction needs higher temperature to be achieved (Fig. 2: 233°C), evidencing a better stabilization of copper species. According to Berger and Roth [38], the observed EPR intensity is a percentage of the theoretical total intensity due to nearly isolated Cu^{2+} ions only. Moreover, Kucherov *et al.* [39] have shown that intensity is correlated with the concentration and the dispersion of the copper (II) species. Using 0.5Cu10Al sample as reference for total dispersion of copper oxide, Table II summarizes the percentage of detected copper species by EPR. Only 19.4 wt% of Cu(II) species is detected by EPR technique for 1Cu10Al sample. However, quantitative TPR results, deduced from H_2 consumption and presented in Fig. 4, show that copper oxide is entirely reduced into Cu^0 (98 wt%). Furthermore, TPR profile of 1Cu10Al shows only one reduction peak. Regarding these results, this peak should be related to clusters reduction, including also the dispersed species reduction peak.

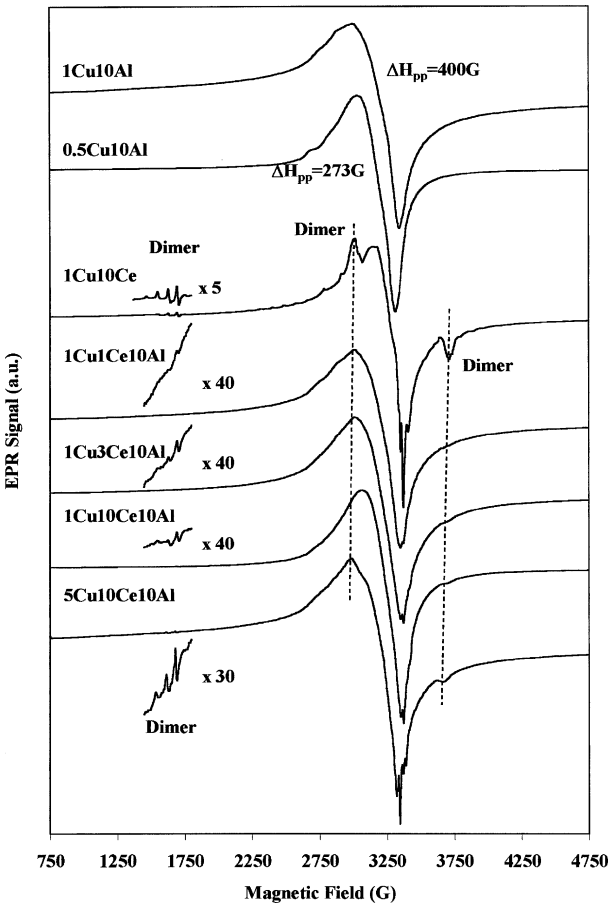

Figure 3 EPR spectra of copper based catalysts recorded at −196°C.

The TPR profile of 1Cu10Ce sample exhibits different peaks (Fig. 2). As for pure ceria, two peaks centered at 594 and 932°C are observed and respectively ascribed to surface and bulk ceria reduction. The temperature of surface ceria reduction of 1Cu10Ce sample (594°C) is considerably lower than that observed in the case of pure CeO_2 (680°C). This phenomenon shows an interaction between copper oxide and ceria surface, which improves ceria reducibility. For ceria bulk, the presence of copper does not change reducibility since temperature of reduction is 940 and 932°C for pure ceria and 1Cu10Ce respectively. In addition to these peaks, a double peak is shown at 150 and 184°C. According to

TABLE II EPR parameters of copper based catalysts spectra recorded at −196°C

Sample	EPR intensity (a.u.)	Dispersion (wt% of CuO per 100 m^2/g of support)	Copper detection (wt% of CuO)	$g_{//}$ monomer	$A_{//}$ monomer (G)
0.5Cu10Al	130.7	1.9	100%	2.346	138
1Cu10Al	62.8	4.7	19.4%	2.326	128
1Cu1Ce10Al	87.8	4.0	31.9%	2.320	128
1Cu3Ce10Al	130.4	3.3	57.4%	2.322	128
5Cu3Ce10Al	89.2	16.2	8.0%	2.317	130
1Cu10Ce10Al	72.5	2.5	42.2%	2.320	133
5Cu10Ce10Al	64.7	11.9	7.9%	2.312	132
1Cu10Ce	157.1	8.4	27.2%	2.295	134

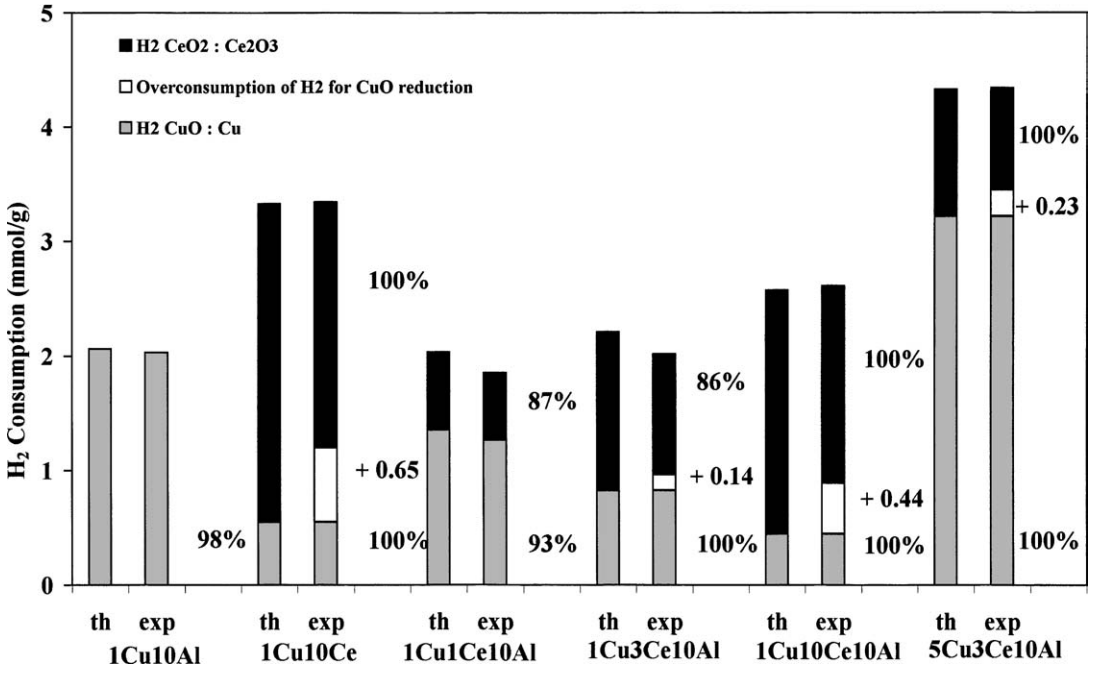

Figure 4 Quantitative results of TPR for copper based catalysts.

Kundakovic and Flytzani-Stephanopoulos [40], when copper content is sufficiently low (2.4 wt% of CuO per gram of catalyst), copper is well dispersed and is only present as isolated copper Cu^{2+} ions or highly dispersed clusters. At higher Cu content (2.4–10.4 wt% of CuO per gram of catalyst), copper is mainly under small clusters. Thus, small clusters are weakly interacting with the support and then are more easily reduced than dispersed species. Reduction peaks of clusters take place at about 160°C. Finally, at higher Cu loading (23.6 wt% of CuO per gram of catalyst), copper is mainly under larger CuO particles, which do not interact with support. In our case, 1Cu10Ce sample contains 4.4 wt% of CuO per gram of catalyst (Table I). Thus, copper can exist under well dispersed copper and cluster form [40]. EPR study shows as for 1Cu10Al sample, an axial signal attributed to Cu^{2+} ions and an isotropic signal related to small clusters (Fig. 3). However, EPR parameters of the axial signal are different from 1Cu10Al sample due to environmental difference ($g_{//} = 2.295; g_{\perp} = 2.047; A_{//} = 134G; A_{\perp} = 39G$). Moreover, a third signal is observed and is attributed to copper (II) ion dimers [37]. This signal displays a fine structure corresponding to the $\Delta m_s = \pm 1$ transition of a triplet state, where two signals with axial symmetries are observed. The EPR parameters of dimers signal are: $g_{//D} = 2.2086; g_{\perp D} = 2.0362; A_{//D} = 86G; A_{\perp D} = 16G$. This signal is observed only for copper in interaction with ceria since dimers are due to 2 copper (II) ions pairs bonded by oxygen formed in ceria [37]. The EPR parameters of this species do not change with solids. Only 27.2% of copper is detected by EPR for 1Cu10Ce sample. Thus copper oxide exists under isolated species (detected by EPR) and clusters form (undetected by EPR). Then, according to literature data and EPR study, the first peak at 150°C is due to the reduction of cluster species weakly interacting with support and the peak centered at 184°C is assigned to isolated Cu^{2+} ions. Furthermore, this study shows that isolated copper species are more easily reducible on ceria than on alumina since similar copper species are reduced at 208°C on 1Cu10Al sample. Alumina presents a high specific area (420 m^2/g), copper is then highly dispersed (4.7 wt% of CuO per 100 m^2/g) and highly stabilized. Thus, dispersed copper on alumina needs high temperature to be reduced. On the contrary, copper on ceria is less stabilized because the dispersion is lower: $\frac{4.4(wt\%)}{0.956\times 55(m^2/g)} = 8.4$ wt% of CuO per 100 m^2/g of support. In addition, ceria has redox properties which enhance the reduction phenomenon [29]. Moreover, a third peak due to copper reduction is observed at 249°C for 1Cu10Ce sample (Fig. 2). This very weak peak is attributed to copper aggregates reduction [13, 30, 40]. Indeed, according to Luo *et al.* [10], the dispersion of copper for 1Cu10Ce sample (Table II) is higher than the limit of aggregates formation. Thus, a part of copper may be under aggregates form.

Fig. 4 shows quantitative results expressed in mmol of H_2 uptake per gram of solid and in percent of CuO or CeO_2 reduced to Cu^0 or Ce_2O_3 respectively. For 1Cu10Ce sample, experimental total hydrogen consumption is quite equivalent to calculated value (3.33 mmol/g), proving that reduction of both copper and ceria is complete. However, the hydrogen consumption ascribed to copper reduction is 0.65 mmol/g higher than calculated value, and ceria reduction shows lower hydrogen consumption (2.14 mmol/g) than calculated one (2.78 mmol/g). These phenomena clearly show that ceria can be partially reduced during copper oxide reduction. Indeed, partial reduction of ceria has been observed in presence of precious metal by a spillover process [1]. In addition, it is well known that dissociative adsorption of hydrogen on copper does not take place easily at low temperature. However, in our case the possibility that the partial reduction of ceria occurs versus hydrogen spillover should not be omitted. This result

is in good agreement with literature data [40] where a partial reduction of ceria during copper reduction, has been observed.

3.2.1. Influence of ceria contents

Concerning Cu–Ce–Al–O mixed oxides, reduction behavior depends on ceria content. Table II shows EPR parameters of copper based catalysts. The $g_{//}$ value depends on solids. This value is 2.326 and 2.295 for 1Cu10Al and 1Cu10Ce respectively. The $g_{//}$ value of Cu–Ce–Al oxides decreases from 2.322 for 1Cu3Ce10Al to 2.320 for 1Cu10Ce10Al (Table II). Moreover, the dimer signal is better defined with increasing of ceria loading (Fig. 3). These observations show that copper oxide is more in interaction with ceria than alumina when ceria content increases. When ceria loading is low (1Cu1Ce10Al and 1Cu3Ce10Al), the major TPR peak is centered at about 230°C and is ascribed to highly dispersed species (Fig. 2). The second peak centered at 190°C, which increases with ceria loading, is due to cluster. Since 1Cu1Ce10Al and 1Cu3Ce10Al solids have high specific areas (Table I), the dispersion is equivalent to 3–4 wt% of CuO per 100 m^2/g of support (Table II), and according to Dow *et al*. [27–29] this dispersion allows to obtain only isolated Cu^{2+} ions and cluster species weakly in interaction with the support. Copper reduction peaks occur at higher temperature for ternary oxides than for 1Cu10Al and 1Cu10Ce. This assertion can be related to the specific area of samples. Indeed, alumina has the most important specific area (420 m^2/g) compared to ceria (55 m^2/g) or copper oxide (8 m^2/g). Thus, when alumina is impregnated by copper or cerium, the loading of alumina decreases and the specific area too. For 1Cu1Ce10Al and 1Cu3Ce10Al samples, the weight percent of alumina is important (65.9 and 45.8 wt% respectively), thus specific area is important too. Table I show specific area measured or calculated from specific area of single oxide. The calculated values (290 and 219 m^2/g for 1Cu3Ce10Al and 1Cu10Ce10Al respectively) are in good agreements with measured values (277 and 192 m^2/g for 1Cu3Ce10Al and 1Cu10Ce10Al respectively) but are slightly higher. This difference can be related to a plugging of alumina micropores by cerium or copper. Cu–Ce–Al–O samples have higher specific area than 1Cu10Ce sample (47 m^2/g). Then, copper is more dispersed and more stabilized on ternay oxides. Moreover, the interaction between copper oxide and ceria is less important, since ceria content is lower. Thus, Cu–Ce–Al–O samples need higher temperature to be reduced than 1Cu10Ce sample. On the other hand, specific areas of 1Cu1Ce10Al and 1Cu3Ce10Al are lower for ternary oxides than for 1Cu10Al sample. Thus, hydrogen adsorption is enhanced for 1Cu10Al than for ternary oxides and Cu–Ce–Al–O oxides need higher temperature to be reduced. Furthermore, quantitative results (Fig. 4) show that for 1Cu1Ce10Al sample, experimental total hydrogen consumption is lower than calculated value, evidencing an incomplete reduction of copper oxide or ceria. Considering H_2 consumption for copper oxide reduction, experimental value is very close to calculated one, proving that copper oxide reduction is almost complete (93%) and consequently, the reduction extent of ceria is about 87% (Fig. 4). It is important to note that ceria reduction extent is higher on the ternary oxide (87%) than on the corresponding support (for 1Ce10Al support, ceria reduction extent is about 68 wt%), showing that the presence of copper species improves the ceria reduction. For 1Cu3Ce10Al, the quantitative results show that the experimental hydrogen used to copper reduction is 0.14 mmol/g higher than calculated value (0.83 mmol/g). This observation can be explained as in the case of 1Cu10Ce sample, by partial reduction of ceria during copper oxide reduction.

For higher ceria containing ternary oxides (1Cu10Ce10Al), TPR profile presented in Fig. 2 exhibits 3 peaks of copper reduction. This solid has the same behavior as 1Cu10Ce. Indeed, the relative support (10Ce10Al) is composed of 75.8 wt% of ceria impregnated on 24.2 wt% of alumina. In these conditions, it can be assumed that alumina is entirely covered by ceria. Consequently, copper is rather on ceria than on alumina. EPR study confirms this assertion since increasing ceria content increases the intensity of the signal related to dimers. As for 1Cu10Ce sample, the first peak (132°C) observed on 1Cu10Ce10Al TPR curve is the reduction peak of cluster weakly interacting with the support. Then, dispersed copper species reduction is observed at 160°C and a third peak is observed at 203°C. Taking into consideration the preparation method of the solid, this latter peak cannot be due to dispersed copper species on alumina, since alumina is covered by ceria. As for 1Cu10Ce sample, this peak is attributed to reduction of copper aggregates. Pure copper oxide is reduced at 290°C [41], but literature data [10, 29, 32, 42] show that CuO aggregates supported by ceria and alumina can be reduced at lower temperature (∼200°C). Furthermore, as for 1Cu10Ce and 1Cu3Ce10Al samples, Fig. 4 shows that hydrogen used for copper reduction in 1Cu10Ce10Al is 0.44 mmol/g higher than calculated value, due to the partial ceria reduction during copper oxide reduction. Moreover, from the data analyzed above showing that hydrogen over-consumption increases with ceria content, it can be deduced that copper-ceria interaction enhances ceria reduction extent. In order to confirm this hypothesis, the influence of copper content is studied.

3.2.2. Influence of copper content

TPR profiles of 1Cu3Ce10Al and 5Cu3Ce10Al (Fig. 2) show that the increase of copper loading leads to a new TPR peak, centered at 297°C. Increasing of copper content for 1Cu10Ce10Al to 5Cu10Ce10Al leads to an increase of the third peak of copper oxide reduction. These assertions are consistent with the attribution of this peak to copper aggregates reduction. EPR data confirm the CuO agglomeration since copper oxide detection decreases from 42.2% for 1Cu10Ce10Al to 7.9% for 5Cu10Ce10Al and from 57.4% for 1Cu3Ce10Al to 8.0% for 5Cu3Ce10Al (Table II). Increasing of copper content leads for all catalysts to higher over-consumption of hydrogen during

copper oxide reduction. The over-consumption of hydrogen observed for 1Cu3Ce10Al is 0.14 mmol H_2/g, whereas for 5Cu3Ce10Al, this over-consumption is 0.23 mmol H_2/g. Thus, the reduction extent of ceria passes from 86 to 100% with the increasing of copper loading (Fig. 4). For higher ceria loading (1Cu10Ce10Al and 5Cu10Ce10Al samples), the over-consumption increases from 0.44 to 0.71 mmol H_2/g. This phenomenon evidences that reduction of ceria during copper reduction is enhances by increasing of copper loading. Moreover, EPR results show an increase of dimer signal intensity and a decrease of $g_{//}$ value (2.322 to 2.317 for 1Cu3Ce10Al and 5Cu3Ce10Al respectively; 2.320 to 2.312 for 1Cu10Ce10Al and 5Cu10Ce10Al respectively) with increasing of copper loading. These TPR and EPR results show that the interaction between ceria and copper species increases with copper loading.

4. Conclusions

The reducibility of Ce–Al–O and Cu–Ce–Al–O solids are studied by H_2-TPR and EPR in order to identify the different ceria and copper oxide species.

The study of Ce–Al–O oxides shows that dispersion of ceria on alumina stabilizes surface ceria and improves the reducibility of bulk ceria. When ceria content increases, reduction temperature of bulk ceria increases, whereas reduction temperature of surface ceria decreases. Simultaneously quantitative results show that ceria reduction extent is more important for Ce–Al–O oxides than for pure ceria.

For ternary oxides, an interaction between copper oxide and ceria is evidenced. Introduction of copper makes ceria reduction easier. Thus ceria is partially reduced during copper reduction (<250°C). Moreover, quantitative results in ternary oxides show that the presence of copper allows a more important or complete reduction of ceria contrary to Ce–Al–O oxides. Copper reduction behavior is influenced by ceria loading in the system. When ceria loading is low, two reduction peaks are observed, and are attributed to small clusters and highly dispersed copper oxides. Increasing of copper loading leads to formation of CuO aggregates, but favors also ceria reduction during copper oxide reduction. These information are useful to know the catalytic ability of these solids for different reactions, such as TWC reactions, or soot combustion.

Acknowledgments

The authors would like to thank the "Conseil Général du Nord," the "Région Nord-Pas de Calais" and the European Community (European Regional Development Fund) for financial supports.

References

1. H. C. YAO and Y. F. YU YAO, *J. Catal.* **86** (1984) 254.
2. E. C. SU and W. G. ROTSCHILD, *ibid.* **99** (1986) 506.
3. A. PIRAS, A. TROVARELLI and G. DOLCETTI, *Appl. Catal. B: Environ.* **28** (2000) L77.
4. S. ROSSIGNOL and C. KAPPENSTEIN, *Intern. J. Mater.* **3** (2001) 51.
5. W. DANIELL, P. GROTZ, H. KNÖZINGER, N. C. LLOYD, C. BAILEY and P. G. HARISSON, *Stud. Surf. Sci. Catal.* **130** (2000) 2183.
6. W. DANIELL, N. C. LLOYD, C. BAILEY and P.G. HARISSON, *Journal de Physique France* **7** (1997) C2-963.
7. A. MARTINEZ-ARIAS, J. SORIA, R. CATALUNA, J. C. CONESA and V. CORTES-CORBERAN, *Stud. Surf. Sci. Catal.* **116** (1998) 591.
8. P. WORN PARK and J. S. LEDFORD, *Appl. Catal. B: Environ.* **15** (1998) 221.
9. *idem.*, *Catal. Lett.* **50** (1998) 41.
10. M. F. LUO, Y. J. ZHONG, X. X. YUAN and X. M. ZHENG, *Appl. Catal. A: Gen.* **162** (1997) 121.
11. F. KAPTEIJN, S. STEGENGA, N. J. J. DEKKER, J. W. BIJSTERBOSCH and J. A. MOULIJN, *Catal. Today* **16** (1993) 273.
12. E. M. CORDI, P. J. O'NEILL and J. L. FALCONER, *Appl. Catal. B: Environ.* **14** (1997) 23.
13. P.-O. LARSSON and A. ANDERSSON, *ibid.* **24** (2000) 175.
14. L. CHEN, T. HORIUCHI, T. OSAKI and T. MORI, *ibid.* **23** (1999) 259.
15. K. W. YAO, S. JAENICKE, J. Y. LIN and K. L. TAN, *ibid.* **16** (1998) 291.
16. Z. CHAJAR, M. PRIMET, H. PRALIAUD, M. CHEVRIER, C. GAUTHIER and F. MATHIS, *Stud. Surf. Sci. Catal.* **96** (1995) 591.
17. C. PRUVOST, J. F. LAMONIER, D. COURCOT, E. ABI-AAD and A. ABOUKAÏS, *ibid.* **130** (2000) 2159.
18. D. COURCOT, E. ABI-AAD, S. CAPELLE and A. ABOUKAÏS, *ibid.* **116** (1998) 625.
19. A. BELLALOUI, J. VARLOUD, P. MERIAUDEAU, V. PERRICHON, E. LOX, M. CHEVRIER, C. GAUTHIER and F. MATHIS, *Catal. Today* **29** (1996) 421.
20. S. YUAN, P. MERIAUDEAU and V. PERRICHON, *Appl. Catal. B : Environ.* **3** (1994) 319.
21. D. W. MCKEE, *Carbon* **8** (1970) 131.
22. *Idem.*, *ibid.* **8** (1970) 623.
23. L. LE BIHAN, C. MAUCHAUSSE, E. PAYEN, L. DUHAMEL and J. GRIMBLOT, *J. Sol-Gel Sci. Technol.* **2** (1994) 837.
24. J. Z. SHYU and K. OTTO, *J. Catal.* **115** (1989) 16.
25. M. HANEDA, T. MIZUSHIMA, N. KAKUTA, A. UENO, Y. SATO, S. MATSUURA, K. KASAHARA and M. SATO, *Bull. Chem. Soc. Jpn.* **66** (1993) 1279.
26. L. G. APPEL, J. G. EON and M. SCHMAL, *Phys. Stat. Sol.* **163** (1997) 107.
27. W. P. DOW and T.-J. HUANG, *Appl. Catal. A: Gen.* **141** (1996) 17.
28. W. P. DOW, Y. P. WANG and T.-J. HUANG, *J. Catal.* **160** (1996) 155.
29. *Idem.*, *Appl. Catal. A: Gen.* **190** (2000) 25.
30. X. COURTOIS, V. PERRICHON, M. PRIMET and G. BERGERET, *Stud. Surf. Sci. Catal.* **130** (2000) 1031.
31. J. M. DUMAS, C. GERON, A. KRIBII and J. BARBIER, *Appl. Catal.* **47** (1989) L9.
32. R. M. FRIEDMAN and J. J. FREEMAN, *J. Catal.* **55** (1978) 10.
33. A. ABOUKAÏS, A. BENNANI, C. F. AISSI, G. WROBEL and M. GUELTON, *J. Chem. Soc. Faraday Trans.* **88** (1992) 1321.
34. A. ABOUKAÏS, A. BENNANI, C. F. AISSI, G. WROBEL, M. GUELTON and J. C. VEDRINE, *ibid.* **88** (1992) 651.
35. R. BECHARA, A. ABOUKAÏS, M. GUELTON, A. D'HUYSSER, J. GRIMBLOT and J. P. BONNELLE, *Spectrosc. Lett.* **23** (1990) 1237.
36. J. SORIA, J. C. CONESA, A. MARTINEZ-ARIAS and J. M. CORONADO, *Solid State Ionics* **63–65** (1993) 755.
37. A. ABOUKAÏS, A. BENNANI, C. LAMONIER-DULONGPONT, E. ABI-AAD and G. WROBEL, *Colloïds and Surf. A: Physicochem. Engineering Aspect* **115** (1996) 171.
38. P. A. BERGER and J. F. ROTH, *J. Phys. Chem.* **71** (1967) 4307.

39. A. V. KUCHEROV, J. L. GERLOCK, H. W. JEN and M. SHELEF, *ibid.* **98** (1994) 4892.
40. LJ. KUNDAKOVIC and M. FLYTZANI-STEPHANOPOULOS, *Appl. Catal. A: Gen.* **171** (1998) 13.
41. Y. HU, L. DONG, J. WANG, W. DING and Y. CHEN, *J. Mol. Catal. A: Chem.* **162** (2000) 307.
42. J. XIAOYUAN, L. GUANGLIE, Z. RENXIAN, M. JIANXIN, C. YU and Z. XIAOMING, *Appl. Surf. Sci.* **173** (2001) 208.

Received 5 June
and accepted 30 December 2003